# THE ROLE OF DIFFUSION WEIGHTED IMAGING IN THE ASSESSMENT OF AXILLARY LYMPH NODES

## AKSİLLER LENF NODLARININ DEĞERLENDİRİLMESİNDE DİFÜZYON AĞIRLIKLI GÖRÜNTÜLEMENİN ROLÜ

Işıl Başara[1], Şebnem Örgüç[2], Teoman Coşkun[3]

[1]Department of Radiology, Faculty of Medicine, Dokuz Eylül University, İzmir, Turkey
[2]Department of Radiology, Faculty of Medicine, Celal Bayar University, Manisa, Turkey
[3]Department of General Surgery, Faculty of Medicine, Celal Bayar University, Manisa, Turkey

Presented In: 32nd National Congress of Radiology National Congress of Radiology

**ABSTRACT**

**Objective:** Several studies have shown that diffusion weighted imaging (DWI) can serve as a powerful tool for differentiating benign from malignant breast lesions. In addition to this use, DWI may also be used in the assessment of axillary lymph nodes, since they show similar tissue characteristics to the primary tumor.

**Materials and Methods:** We applied dynamic contrast enhanced breast magnetic resonance imaging and DWI to 110 female patients and 214 breasts. Apparent diffusion coefficient (ADC) values of 187 lymph nodes (142 benign and 45 malignant) in 177 axillae were measured. Malignant lymph nodes were diagnosed histopathologically, benign lymph nodes were diagnosed clinically and with imaging findings.

**Results:** The mean ADC values were $1.00 \times 10^{-3}$ mm$^2$/s for the malignant, and $1.39 \times 10^{-3}$ mm$^2$/s for the benign lymph nodes. The ADC values of malignant lymph nodes were significantly lower than the benign ones (p=0.001). When $1.22 \times 10^{-3}$ mm$^2$/s was accepted as the cut-off ADC value, a sensitivity of 75.6% and a specificity of 71.1% were detected.

**Conclusion:** Our preliminary data suggest that ADC measurements might be useful in differentiating malignant from benign axillary lymph nodes in the preoperative period. Further studies on a larger scale will increase confidence in the results of DWI.

**Key words:** Diffusion weighted, magnetic resonance imaging, breast cancer, lymph nodes

**ÖZET**

**Amaç:** Pek çok çalışma difüzyon ağırlıklı görüntülemenin (DAG) malign meme lezyonlarının benign lezyonlardan ayırmada güçlü yöntem olduğunu göstermiştir. Bu kullanıma ek olarak, primer tümörle benzer doku karakteristiğine sahip olduğundan DAG, aksiller lenf nodlarının değerlendiriminde de kullanılabilir.

**Yöntem ve Gereçler:** Yüz on kadın hasta ve 214 meme dokusunda, kontrastlı dinamik manyetik rezonans görüntüleme ve DAG uyguladık. Yüz yetmiş yedi aksillada, 187 lenf nodunda (142 benign ve 45 malign) Apparent diffusion coefficient (ADC) değerleri ölçüldü. Malign lenf nodu tanısı histopatolojik olarak, benign lenf nodu tanısı klinik ve görüntüleme bulguları ile konuldu.

**Bulgular:** Ortalama ADC değerleri, malign lenf nodları için $1.00 \times 10^{-3}$ mm$^2$/s, benign lenf nodları için $1.39 \times 10^{-3}$ mm$^2$/s'dir. Malign lenf nodlarında ADC değerleri benign olanlardan belirgin düşüktür (p=0.001). Cut-off ADC değeri $1.22 \times 10^{-3}$ mm$^2$/s Kabul edildiğinde, sensitivite %75.6 ve spesifisite %71.1 olarak hesaplandı.

**Sonuç:** Ön bulgularımıza göre, preoperatif dönemde malign ve benign aksiller lenf nodlarının ayrımında ADC ölçümlerinin kullanışlı olabileceğini önermektedir. Geniş serilerle yapılan ileri çalışmalar DAG'deki sonuçlara güveni arttıracaktır.

**Anahtar sözcükler:** Difüzyon ağırlıklı, manyetik rezonans görüntüleme, meme kanseri, lenf nodu

Lymph node metastasis is one of the most important prognostic factor in breast cancer. Preoperative prediction of the axillary nodal status remains an important challenge in the management of patients. Diffusion weighted imaging (DWI) is an advanced magnetic resonance imaging (MRI) application which derives its image contrast from the differences in water mobility in the extracellular spaces, reflecting cellular density, organization, microstructure and microcirculation.

Several studies have shown that DWI can serve as a powerful tool for differentiating benign from malignant breast lesions. In addition to this use, DWI may also be used in the assessment of axillary

lymph nodes, since they show similar tissue characteristics to the primary tumor (1, 2).

Evaluation of lymph nodes is a promising novel application of DWI, which can easily be applied as an adjunct to conventional breast MRI. There are a few preliminary studies that have shown that DWI can be used to detect lymph nodes affected by malignant cells. Koh et al. report that after the involvement of nodes with malignancy, they undergo changes and the increase in cellularity leads to diffusion restriction and low apparent diffusion coefficient (ADC) values (1). Eiber et al. reported that DWI has a potential for the characterization of pelvic lymph nodes in patients with prostate cancer in their retrospective study (2).

In this study we aimed to evaluate ADC values of axillary lymph nodes and the contribution of DWI to the diagnosis of malignant axillary lymph node involvement.

**Materials and Methods**
We applied dynamic contrast enhanced breast MRI and DWI using a 1.5 Tesla MR device (Signa HDx; General Electric, WI, USA) and bilateral 8-channel high density breast coil to 110 female patients who were prospectively enrolled in the study with various indications of conventional breast MRI between November 2009-July 2011. The number of breast and axillae included in the study was 214. Six patients had unilateral mastectomy and axillary dissection. As a result, 6 operated axillae were not included in the study. The study was approved by the local ethics committee, and all patients provided written informed consent.

The standard sequences for conventional breast MRI were axial Short Tau Inversion Recovery (STIR), sagittal Fast Spin Echo Fat Saturated T2W and sagittal 3D VIBRANT (Postcontrast Dynamic Fat Saturated T1W sequence optimized for breast imaging). DWI with b=0 s/mm$^2$ and b=600 s/mm$^2$ values were applied in the axial plane prior to application of contrast material. The other parametric values for DWI were as follows: Sequence EPI, TR/TE 7900 ms/88.9 ms (minimum TE), FOV 36-40mm, matrix 192x192, slice thickness/interval: 5 mm/1 mm, NEX 16, rBW 250 kHz, scan time 261 s.

After acquisition, all data were transferred to a Workstation (Advantage Windows 4.4). During postprocessing, black and white Apparent Diffusion Coefficient (ADC) maps were generated. First, the axillary lymph nodes were located on the axial STIR and postcontrast T1W images. Second, their locations were correlated with the diffusion weighted images and ADC maps. Next, ADC values of all visible axillary lymph nodes were measured. The nodes were determined by consensus of the two radiologists.

A total of 177 axillae and 187 lymph nodes (2 nodes in 6, and 3 nodes in 2 axillae) were included in the study. No measurable lymph node was detected in 37 axillae. The sizes of the lymph nodes were determined by measuring the longest diameter (equal and/or larger than 8mm). The ROI was placed over the lymph node, trying to avoid the fatty hila of the axillary lymph nodes. Sizes of the region of interest (ROI) varied between 10-100mm$^2$. The ROC analysis of the data was evaluated and the area under the curve was calculated. Additionally, the cut-off ADC values to differentiate benign and malignant axillary lymph nodes were calculated. The findings were compared with the histopathological results and final diagnosis of the patients. To ensure that the lymph nodes

ADC measurements obtained were the same as the ones dissected in surgery, they were discussed with the pathologist and the surgeon. The maximum diameters of the lymph nodes were correlated with the pathology specimen.

Results were evaluated statistically by using the SPSS 16.0 for Windows version. The overall statistical differences between mean values were evaluated with the student's *t* test for matched pairs. *P* values less than 0.05 were considered to indicate a statistically significant difference. Receiver operating characteristic (ROC) analysis was performed in order to determine the diagnostic capability of DWI and cut-off ADC value with optimal sensitivity and specificity
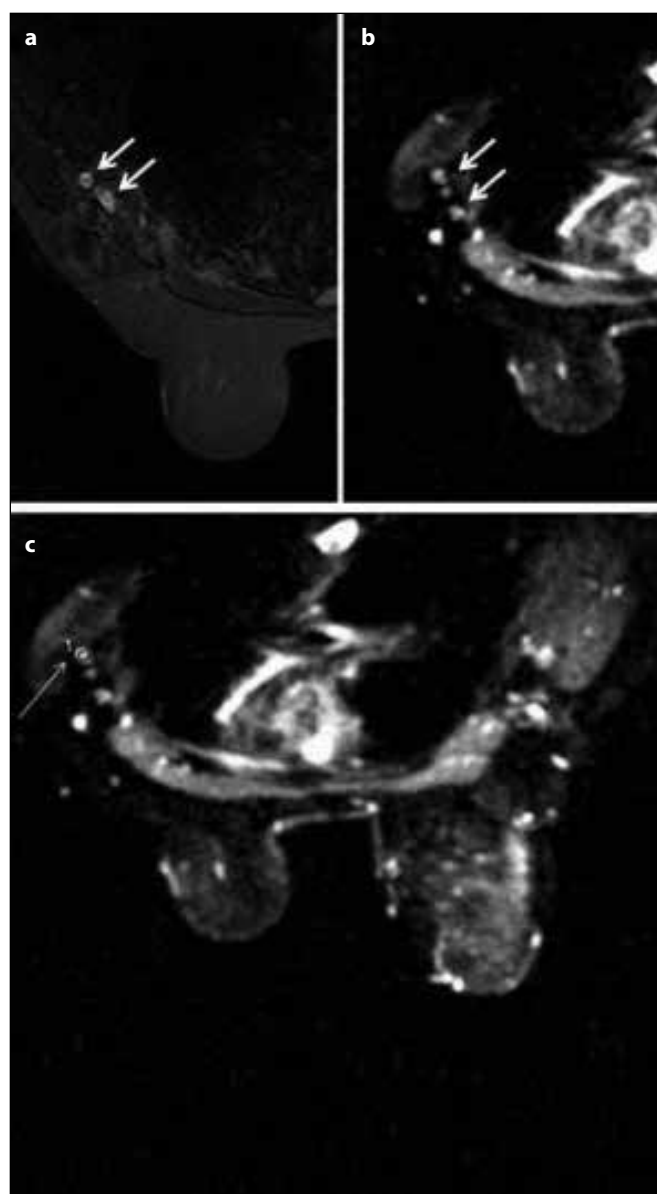


**Figure 1.** Nineteen-year-old woman with congenital hypoplasia of left breast, and otherwise normal MRI examination. Benign reactive axillay lymph nodes are also demonstrated. **a.** Axial STIR image, multiple reactive left axillary lymph nodes with fatty hila (arrows). **b, c.** In ADC map, the lymph node is hyperintense and the ADC value of left axillary lymph node is measured 1.42x10$^{-3}$mm$^2$/sec (arrows).
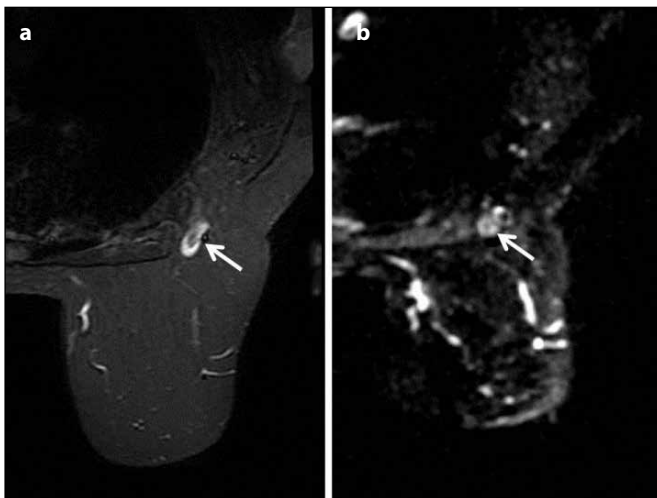
**Figure 2.** Fifty-one-year-old female with invasive ductal carcinoma on the contra-lateral (left) breast. **a.** Axial STIR image, reactive right axillary lymph nodes with fatty hilum (arrows). **b.** In ADC map, ADC value of hyperintense right axillary lymph node is measured 1.68x10$^{-3}$mm$^2$/sec (arrows). ROI is placed taking care not to include the fat in the hilum of the lymph node.

levels and highest accuracy in differentiating benign and malignant axillary lymph nodes.

## Results

There were 142 benign, and 45 malignant lymph nodes. Malignant lymph nodes were diagnosed histopathologically, benign lymph nodes were diagnosed clinically and with imaging findings. The median age (range 19-73) was 47 years for the benign, and 43 (range 29-70) years for the malignant group. The ages were not significantly different in the two groups (p=0.3). On histopathological examination, 45 of the axillary lymph nodes proved to be malignant in 40 patients (invasive ductal carcinoma (IDC; n:31), invasive lobular carcinoma (ILC; n:1), mixed invasive lobular and ductal carcinoma (n:3), mixed IDC + mucinous carcinoma (n:1), IDC+pleomorphic carcinoma (n:1), medullary carcinoma (n:1), and malignant phyllodes tumor (n:1), diffuse leukemic infiltration of the breast (n:1)

The ADC measurements of a total of 142 lymph nodes in 137 patients were included in the benign group of the study. The lymph nodes detected in patients with a final diagnosis of no breast cancer and in patients with known malignancy and with benign contrlateral axillary lymph nodes were included in the benign lymph node group.

The mean diameter of the malignant lymph nodes was 17.1 mm (Standard deviation: 8.2 mm), the mean diameter of the benign lymph nodes was 11.3 mm (Standard deviation: 3.3 mm). The malignant axillary lymph nodes were significantly larger than the benign ones (p=0.001).

The mean ADC value for the malignant lymph nodes was 1.00x10$^{-3}$ mm$^2$/s. (Standard deviation 0.30x10$^{-3}$ mm$^2$/s). The mean ADC value for the benign lymph nodes was 1.39 x10$^{-3}$ mm$^2$/s. (Standard deviation 0.30x10$^{-3}$ mm$^2$/s). The ADC values of malignant lymph nodes were significantly lower than the benign ones (*p*=0.001). Represen-
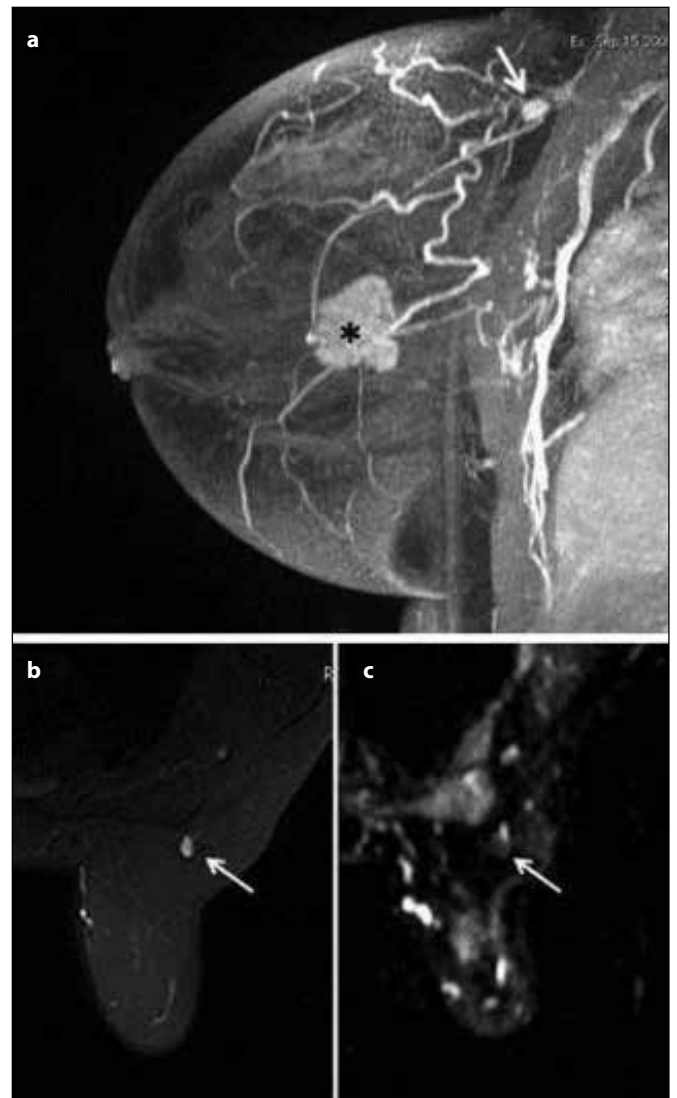


**Figure 3.** A 55-year-old woman, with invasive ductal carcinoma of the right breast and axillary lymph node metastasis. **a.** Sagital 3D MIP vibrant image, shows a spiculated malignant breast tumor (asterisk) and a small lymph node in the ipsilateral axilla (arrow). **b.** Axial STIR image, demonstrating the lymph node with no fat in the hilum (arrow). **c.** ADC map, lymph node is hypointense and ADC value is measured 0.68x10$^{-3}$mm$^2$/sec (arrow).

tative cases of the study are presented in figures 1-6 (Figure 1-6). In the figures, the benign lymph node had a fatty hilus with an ovoid shape. Mostly they have lower dimensions. The ADC values were lower than those of the malignant ones. The dimensions in malignant nodes were higher and they have spherical shapes without a fatty hilum.

The ROC analysis of the ADC values of axillary lymph nodes was evaluated (Figure 7) and the ADC values of benign and malignant lymph nodes were determined to be significantly different from each other. The area under the curve was 0.814, with a standard deviation of 0.38 (95% confidence interval of 0.739-0.888) (p<0,001). This means that the DWI measurement is quite predictive for malignant LAP.

**Table 1.** Histopathological evaluation of lymph nodes and comparison with DWI results.

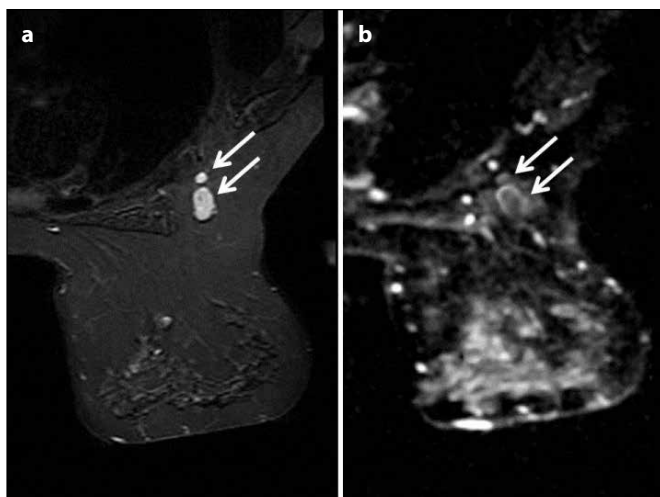| Cut off value | Histopathology/ DWI | | | | Sensitivity | Specificity | Positive predictive value | Negative predictive value |
|---|---|---|---|---|---|---|---|---|
| | +/+ | +/- | -/+ | -/- | | | | |
| <1.22 x10$^{-3}$ mm$^2$/s | 34 | 11 | 41 | 101 | 75,6% | 71,1% | 45,3% | 90,2% |
| <1.49 x10$^{-3}$ mm$^2$/s | 43 | 2 | 99 | 43 | 95,6% | 30,3% | 30,3% | 95,6% |



**Figure 4.** A 50-year-old woman, with right sided invasive ductal carcinoma, and two axillary lymph node metastases. **a.** Axial STIR image, showing two hyperintense lymph nodes, one of which is very small (arrows). **b.** ADC map, lymph node is hypointense and ADC value is measured 0.82x10$^{-3}$mm$^2$/sec.

When 1.22 x10$^{-3}$ mm$^2$/s was accepted as the cut-off ADC value, a sensitivity of 75.6% and a specificity of 71.1% were detected. However, if a sensitivity of 95.6%, with a cut-off ADC value of 1.49 x10$^{-3}$ mm$^2$/s were used, the specificity was considerably low (31.3%). Thirty seven axillae with no lymph in this study were not determined in the sensitivity-specificty calculation. In the Table, DWI results and histopathologic evaluation of lymph nodes are shown (Table 1). In the content of this study, the correlation between ultrasonography and positron emmision tomography was notmade. This correlation may be determined in further studies.

## Discussion and Conclusion

Breast MRI is an established method in the diagnosis and staging of breast carcinoma (3-6). In conventional breast MRI, tissues can be differentiated from each other according to their T1 and T2 signal features and enhancement characteristics. However, in some cases, especially if no contrast material is used, T1 and T2 features of the tissues are insufficient to differentiate their nature. Diffusion MRI is an imaging method which uses a totally different source of signal. The contrast of this imaging method depends on the molecular motion of the water in the tissues at a microscopic level (7, 8). Diffusion occurs as a result of random thermal waving and this is termed "Brownian motion" (9-11). DWI is a primary imaging method which is used in the diagnosis of cerebral infarction. Recently, however it has been used to evaluate other organs such as ovaries, pancreas, prostate and breast (5,10-17).

There are several studies about discrimination of breast masses with DWI techniques in the literature (10-13). With regard to its clinical usability, DWI can easily and quickly be performed as an adjunct to conventional breast MRI. During breast MRI, T1W and T2W images
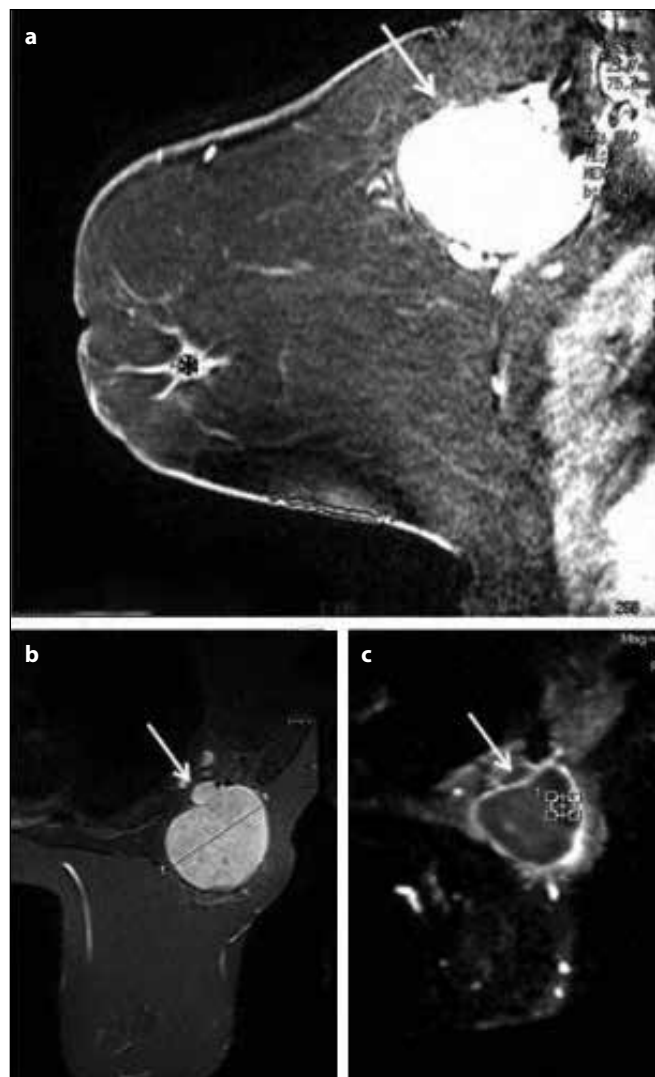


**Figure 5.** Thirty-eight-year-old woman with small invasive ductal carcinoma in the right breast. There are multiple, giant axillary lymph nodes. **a.** Sagittal post-contrast VIBRANT image, there is a giant enhancing lymph node in the right axilla (arrow). Small invasive ductal carcinoma is at the lower quadrant of the right breast (asterisk). **b.** In axial STIR image, there are multiple large hyperintense axillary lymph nodes. (arrow). **c.** In ADC map, the lymph node is hypointense (arrow). ADC value is measured as 0.62x10$^{-3}$mm$^2$/s.

are routinely obtained before dynamic enhanced examination. Biological characteristics of tissues as well as breast masses can be determined using DWI (9). DWI has a potential to replace T2W imaging because b:0 s/mm$^2$ value is essential in a T2W image and it also has a topographic role. DWI can also be used in patients with a history of contrast material allergy. High contrast material costs and risk of nephrogenic systemic fibrosis (NSF) are potential factors which will
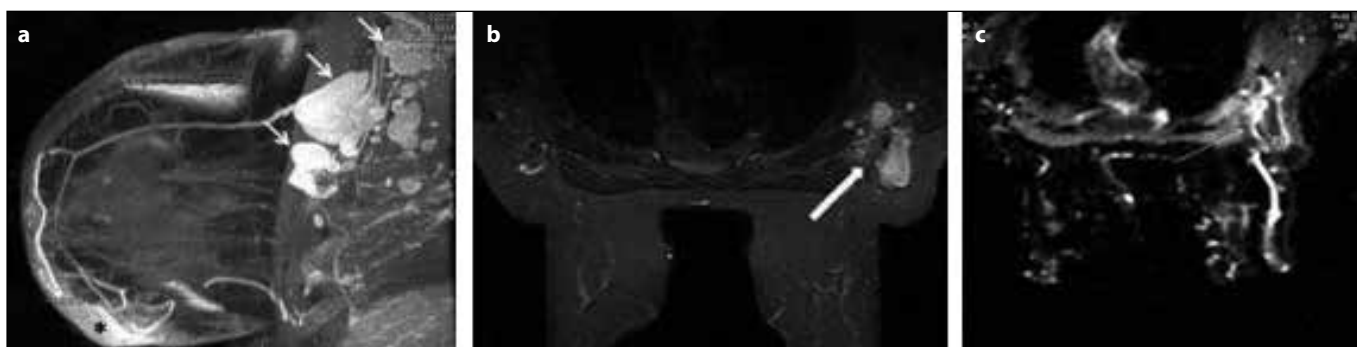
**Figure 6.** Fifty-five-year-old woman with nonspecific abscess of the right breast. There are multiple, giant axillary lymph nodes. **a.** Sagital MIP image, there are multiple enhancing lymph nodes (arrows). Abscess of the right breast located in the subcutaneous tissues of the lower quadrant (asterisk). **b.** In axial STIR image, there are multiple large hyperintense lymph nodes. (arrows). **c.** In ADC map, the lymph node is hypointense (arrows). ADC value is measured as $0.58 \times 10^{-3}$ mm$^2$/s
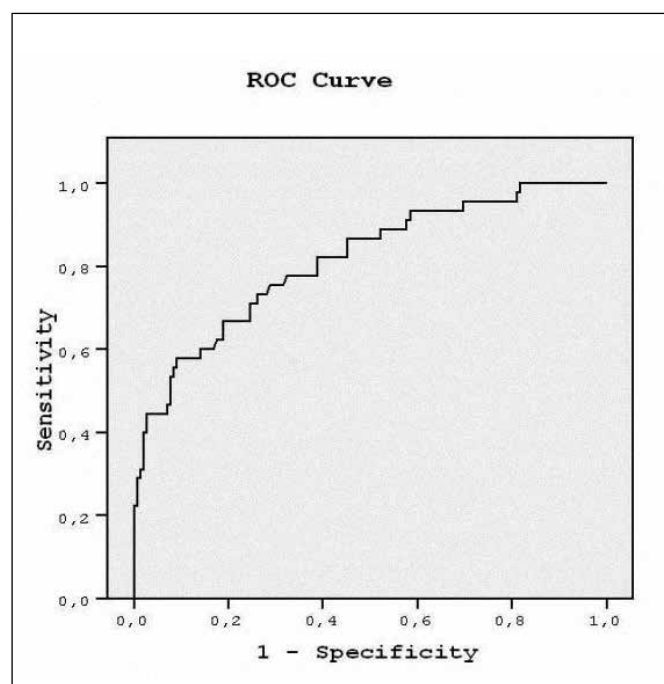


**Figure 7.** Receiver operating characteristic (ROC) curve of ADC values of malignant and benign axillary lymph nodes plotted in the graph of 1- sensitivity versus specificity. The area under the curve is 0.814 with a standard deviation of 0.38 (95% confidence interval of 0.739-0.888).

influence the usage of DWI instead of dynamic breast MRI in the future when consistent results with high accuracy is reached.

In malignant tumors, as a result of high cellular density, there are low ADC values with restricted diffusion in DWI. In benign tumors, because of low cellular density, diffusion restriction is not seen in DWI and high ADC values are measured. The reason for restricted diffusion in DWI is limitations of water molecules motion as a result of high cellularity around, intracellular and extracellular edema, high viscosity and high levels of fibrosis (1,5,18).

In biological tissues ADC expression is used instead of the diffusion coefficient. Since in vivo measured signal loss is different from in vitro measured signal loss in general, microscopic motions in biological tissues contain both molecular diffusion and microcirculation of blood in capillary vessels. Both diffusion and perfusion affect

ADC values. Low b value images result in less diffusion weighted images, since a lower gradient is applied. Also, the extension of microvascular structures in the malignant masses increase the perfusion effect on the ADC values with low b values (9,14,19). However the signal to noise ratio is higher than the high b value diffusion images. The variations of the ADC values between the previous reports can be explained mainly by different b-values (0-1074 s/mm$^2$), other technical factors and variations of the pathologies included in the series. Typically, at least, two b values must be used during DWI in order to enable a meaningful ADC interpretation. However, the accuracy increases when more b values are used. Woodhams et al report that b values less than 750mm$^2$/sec are highly efficient in detecting breast masses (14). Pereira et al reported no significant difference between the ADC values of benign and malignant lesions when different b-value combinations are used, and concluded that using multiple b-values in the DWI sequence is unnecessary (20). Therefore, we used b values of 0 and 600s/mm$^2$ in our study in order to save examination time.

A highly significant difference between the mean ADC values of malignant versus benign lymph nodes was detected in our study (p value: 0.001). When $1.22 \times 10^{-3}$ mm$^2$/s was accepted as the cut-off ADC value, a sensitivity of 75.6% and specificity of 71.1% were detected. However, with a sensitivity of 95.6%, and a cut-off ADC value of $1.49 \times 10^{-3}$ mm$^2$/s, the specificity was considerably low (31.3%).

Although there are several studies reporting various ADC values for breast lesions, there is no specific study on the ADC values of malignant axillary lymph nodes (6-9). In their study of the pelvic lymph nodes of patients with prostate cancer, Eiber et al report a highly significant difference between the mean ADC values (x10$^{-3}$ mm$^2$/s) of malignant ($1.07 \pm 0.23$) versus benign ($1.54 \pm 0.25$) lymph nodes, ADC-value for differentiation of malignant and benign lymph nodes at a cut off $1.30 \times 10^{-3}$ mm$^2$/s with a sensitivity of 86.0% and specificity of 85.3% (2). Their findings indicate that DWI is an accurate and feasible technique for the analysis of pelvic lymph nodes. Therefore, we predict that malignant axillary lymph nodes should have similar restricted diffusion and correspondingly low ADC values.

To ensure accurate nodal evaluation, the potential pitfalls of DWI must be kept in mind. Inclusion of the necrotic areas and fatty hilum of the nodes are possible sources of error in ADC measurements. Inflammatory nodal hyperplasia accompanied by increased cellu-

larity and nodal heterogeneity remain limitations of DWI evaluation of nodal disease. Technical improvements in diffusion weighted imaging and increased spatial resolution overcomes most of the drawbacks and limitations and enables nodal characterization. Quick application time and lack of need for administration of exogeneous contrast material are the major advantages of DWI. Reviewing the DWI findings in conjunction with the morphological findings, accurate anatomical localization and correlation of radiologic findings with the histopathology will increase the success of DWI. High cellular density of the malignant lymph nodes results in restricted diffusion, which may even be detected in normal sized lymph nodes. Measuring the ADC values provides a valuable tool in the preoperative assessment of lymph node status based on cut-off values. However they must be interpreted cautiously, because of the various cut-off values reported for malignancy in the literature. It must also be kept in mind that the optimum cut-off for ADC values has to be determined for each MRI unit, because of the variations in the hardware and pulse sequences.

It is unclear whether DWI can accurately diagnose small metastases, let alone micrometastases. Determination of the necessary lymph nodal invasion ratio required to restrict diffusion, and thus reduce the ADC value, is needed for successful clinical applications. Nevertheless, DWI can reduce the number of sentinel lymph node studies by detecting the malignant nature of the lymph nodes preoperatively. In the future, if the investigations increase, the lymph nodes which could not have been determined without the need of contrast material administration can be determined. This possibility can lead us to decrease the number of sentinel lymph node biopsy. With this method, which has lower dependence on user compared to ultrasonography, will be able to increase the accuracy. Further studies with a large number of subjects will increase confidence in the results of DWI and guide physicians involved in diagnosis, treatment and follow up of breast cancer patients.

## Conflict of interest

No conflict of interest was declared by the authors.

## References

1. Koh DM, Collins DJ. Diffusion-weighted MRI in the body: applications and challenges in oncology. AJR Am J Roentgenol 2007; 188: 1622-35. (PMID: 17515386) **[CrossRef]**
2. Eiber M, Beer AJ, Holzapfel K, Tauber R, Ganter C, Weirich G, et al. Preliminary results for characterization of pelvic lymph nodes in patients with prostate cancer by diffusion-weighted MR-imaging. Invest Radiol 2010; 45: 15-23. (PMID: 19996762) **[CrossRef]**
3. Orel SG, Schnall MD. MR imaging of the breast for the detection, diagnosis, and staging of breast cancer. Radiology 2001; 220: 13-30. (PMID: 11425968)
4. DeBruhl ND, Michael D, Basset LW. Magnetic resonance imaging of breast tunors. In: Basset LW, Jackson VP, Fu KL, Fu YS, eds. Diagnosis of Diseases of the Breast 2nd ed. Elsevier Saunders: Philadelphia, 2005; 225-250.
5. Bluemke DA, Gatsonis CA, Chen MH, DeAngelis GA, DeBruhl N, Harms S, et al. Magnetic resonance imaging of the breast prior to biopsy. JAMA 2004; 292: 2735-42. (PMID: 15585733) **[CrossRef]**
6. Ikeda DM, Baker DR, Daniel BL. Magnetic resonance imaging of breast cancer : clinical indications and breast MRI reporting system. J Magn Reson Imaging 2000; 12: 975-83. (PMID: 11105039) **[CrossRef]**
7. Schaefer PW, Grant PE, Gonzales RG. Diffusion-weighted MR imaging of the brain. Radiology 2000; 217: 331-45. (PMID: 11058626)
8. Gray L, MacFall J. Overview of diffusion imaging. Magn Reson Imaging Clin N Am 1998; 6:125-38. (PMID: 9449744)
9. Bammer R. Basic principles of diffusion-weighted imaging. Eur J Radiol 2003; 45: 169-84. (PMID: 12595101) **[CrossRef]**
10. Guo Y, Cai YQ, Cai ZL, Gao YG, An NY, Ma L, et al. Differentiation of clinically benign and malignant breast lesions using diffusion-weighted imaging. J Magn Reson Imaging 2002; 16: 172-8. (PMID: 12203765) **[CrossRef]**
11. Sinha S, Lucas-Quesada FA, Sinha U, DeBruhl N, Bassett LW. In vivo diffusion-weighted MRI of the breast: potential for lesion characterization. J Magn Reson Imaging 2002; 15: 693-704. (PMID: 12112520) **[CrossRef]**
12. Kinoshita T, Yashiro N, Ihara N, Funatu H, Fakuma E, Narita M. Diffusion-weighted half-Fourier single-shot turbo spin echo imaging in breast tumor: differentiation of invasive ductal carcinoma from fibroadenoma. J Comput Assist Tomogr 2002; 26: 1042-6. (PMID: 12488758) **[CrossRef]**
13. Woodhams R, Matsunaga K, Iwabuchi K, Kan S, Hata H, Kuranami M, et al. Diffusion-weighted imaging of malignant breast tumors: the usefulness of apparent diffusion coefficient (ADC) value and ADC map for the detection of malignant breast tumors and evaluation of cancer extension. J Comput Assist Tomogr 2005; 29: 644-9. (PMID:16163035) **[CrossRef]**
14. Kim T, Murakami T, Takahashi S, Hori M, Tsuda K, Nakamura H. Diffusion-weighted single-shot echoplanar MR Imaging for liver disease. AJR Am J Roentgenol 1999; 173: 393-8. (PMID: 10430143) **[CrossRef]**
15. Yamashita Y, Namimoto T, Mitsuzaki K, Urata J, Tsuchigame T, Takahashi M, et al. Mucin-producing tumor of the pancreas: diagnostic value of diffusion-weighted echo-planar MRI imaging. Radiology 1998; 208: 605-9. (PMID: 9722835)
16. Moteki T, Ishizaka H. Diffusion-weighted EPI of cystic ovarian lesions: evaluation of cystic contents using apparent diffusion coefficients. J Magn Reson Imaging 2000; 12: 1014-9. (PMID: 11105044) **[CrossRef]**
17. Hosseinzadeh K, Schwarz SD. Endorectal diffusion-weighted imaging in prostate cancer to differentiate malignant and benign peripheral zone tissue. J Magn Reson Imaging 2004; 20: 654-61. (PMID: 15390142) **[CrossRef]**
18. Woodhams R, Matsunaga K, Kan S, Hata H, Ozaki M, Iwabuchi K. ADC mapping of benign and malignant breast tumors. Magn Reson Med Sci 2005; 4: 35-42. (PMID: 16127252) **[CrossRef]**
19. Ichikawa T, Haradome H, Hachiya J, Nitatori T, Araki T. Diffusion-weighted MR imaging with a single-shot echoplanar sequence: detection and characterization of focal hepatic lesions. AJR Am J Roentgenol 1998; 170: 397-402. (PMID: 9456953) **[CrossRef]**
20. Pereira FP, Martins G, Figueiredo E, Domingues MN, Domingues RC, da Fonseca LM, et al. Assessment of breast lesions with diffusion-weighted MRI: comparing the use of different b values. AJR Am J Roentgenol 2009; 193: 1030-5. (PMID: 19770326) **[CrossRef]**

*Correspondence / Yazışma Adresi*

Işıl Başara
Phone      : +90 (232) 412 22 22
E-mail     : slbasara@yahoo.com